Supporting Information

Synergetic Modulating the Electronic Structure and Hydrophilicity of Nickel-Iron Hydroxide for Efficient Oxygen Evolution by UV/Ozone Treatment

Ying Pan,[a] Yanfang Wu,[b] H. Alex Hsain,[c] Ran Su,[d,□] Claudio Cazorla[a] and Dewei Chu[a,□]

[a] *School of Materials Science and Engineering, University of New South Wales, 2052, Australia*

[b] *School of Materials Chemistry, University of New South Wales, 2052, Australia*

[c] *Materials Science and Engineering, North Carolina State University, 27695, USA*

[d] *College of Science, Hebei University of Science and Technology, 050018, China*

□ *Corresponding author: d.chu@unsw.edu.au (D. Chu) suranxida@163.com (R. Su)*

Experimental Procedure

Materials: Experimental Details. Nickel nitrate ($Ni(NO_3)_2{\cdot}6H_2O$, M_w: 290.81), iron nitrate ($Fe(NO_3)_3{\cdot}9H_2O$, M_w: 403.99), urea (M_w: 60.04), 1,2-propanediol (ρ: 1.036 g/mL), and carbon paper (Fuel Cell Store).

Synthesis of nickel hydroxides and Ni-Fe hydroxides: The synthesis of nickel hydroxide named as Ni-OH was reported in our previous study.[1] Typically, 0.5 mmol $Ni(NO_3)_2{\cdot}6H_2O$ was dissolved into 2.5 mL deionized (DI) water to obtain a green solution. Afterwards, 10 mL 1,2-propanediol and 0.12 g urea were added into the solution respectively. Then the mixed solution was transferred into a Teflon container and heated in an autoclave at 150 °C for 12 h. After cooling down to room temperature, the as-synthesized product was collected by washing using DI water and drying at 80°C for 24 h. The synthesis of Ni-Fe hydroxide named as NiFe-OH is similar to that of nickel hydroxide except replacing 0.5 mmol $Ni(NO_3)_2{\cdot}6H_2O$ by 0.24 mmol $Ni(NO_3)_2{\cdot}6H_2O$ and 0.06 mmol $Fe(NO_3)_3{\cdot}9H_2O$. The best catalytic parameter (the atomic ratio of Fe/Ni) of the Fe-Ni complex was proven to be 1/4.[2]

UV/Ozone treatment: For the preparation of a working electrode, 5 mg catalysts (Ni-OH, NiFe-OH) were first dispersed in a mixture containing 500 µL water, 450 µL ethanol and 50 µL 5 wt% Nafion. After sonication for 30 min to form a homogeneous ink, 50 µL ink was pipetted onto the carbon paper (mass loading: 1 mg cm^{-2}) and the electrode was dried at room temperature overnight. The UV/ozone treatment procedure was similar to our previous work.[3] Briefly, the prepared working electrodes were treated under UV irradiation using a UV/ozone surface processor (Sen Lights Corporation, Japan) for 120 min (Fig. S1). And samples after UV/Ozone treatment are named as UV-Ni-OH and UV-NiFe-OH, respectively.

Materials characterization: The crystal structures of the catalysts were evaluated by X-ray diffraction (XRD) (MPD PANalytical Xpert multipurpose X-ray diffraction system using filtered Cu Kα radiation, λ = 0.1541 nm). The morphology was observed by scanning electron microscopy (SEM, FEI Nova NanoSEM 450) and transmission electron microscopy (TEM, Philips CM200). The thickness of NSs was measured by atomic force microscopy (AFM, Bruker) using ScanAsyst probe. The chemical compositions and surface element states were determined by X-ray photoelectron spectroscopy (XPS, ESCALAB250Xi spectrometer). Contact angles with Milli-Q water were measured by the sessile drop method using Ramé-Hart 200-F1 goniometry under room temperature. A 6 µL droplet is employed for the static contact angle measurement each time. BET specific surface area was measured at 77 K with a Micromeritics TriStar.

Electrode preparation and electrochemical tests: All the electrochemical tests were carried out in a three-electrode system (1 M KOH) at room temperature using Autolab PGSTAT302 N. Platinum plate, the Ag/AgCl (saturated KCl solution) and catalysts loaded carbon paper was used as the counter electrode, the reference electrode and the working electrode, respectively. The potentials were calibrated against to reversible hydrogen electrode (RHE) by the equation: E_{RHE} = E(Ag/AgCl) + 0.197 V + 0.059 × pH. Linear sweep voltammograms (LSVs) were measured from 1.023 V to 1.823 V vs. RHE for OER with the scan rate of 5 mV s^{-1}. The electric double-layer capacitance (C_{dl}) was calculated by conducting cyclic voltammograms (CVs) from 0.923V to 1.023 V *vs*. RHE at different scanning rates from 10 to 100 mV s^{-1}. Electrochemical impedance spectroscopy (EIS) was measured at a potential of 1.673 V *vs*. RHE over a frequency ranging from 0.1 Hz to 10 kHz. Chronopotentiometric durability was recorded at a constant current density of 30 mA cm^{-2}.

Fig. S1 Apparatus for UV/Ozone treatment.

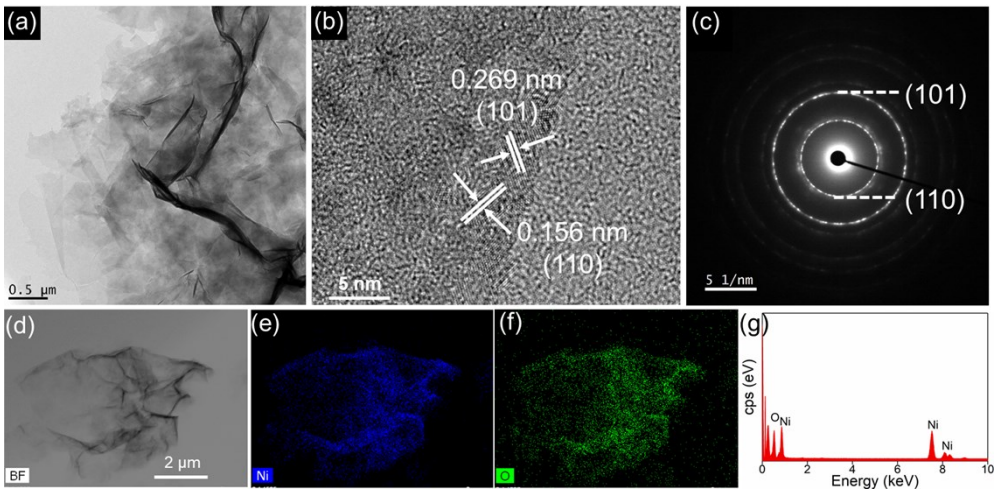

Fig. S2 (a) TEM, (b) HRTEM images and (c) SEAD patterns of Ni-OH. EDX elemental mapping of Ni-OH: (d) bright-field image, (e) Ni, (f) O and (g) the corresponding EDX spectrum.

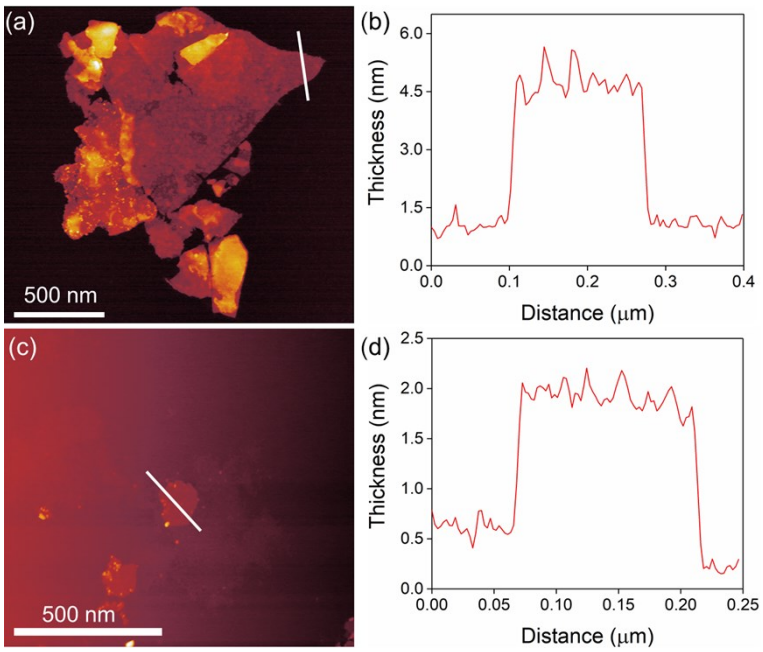

Fig. S3 AFM images and thickness profiles of (a, b) Ni-OH and (c, d) NiFe-OH.

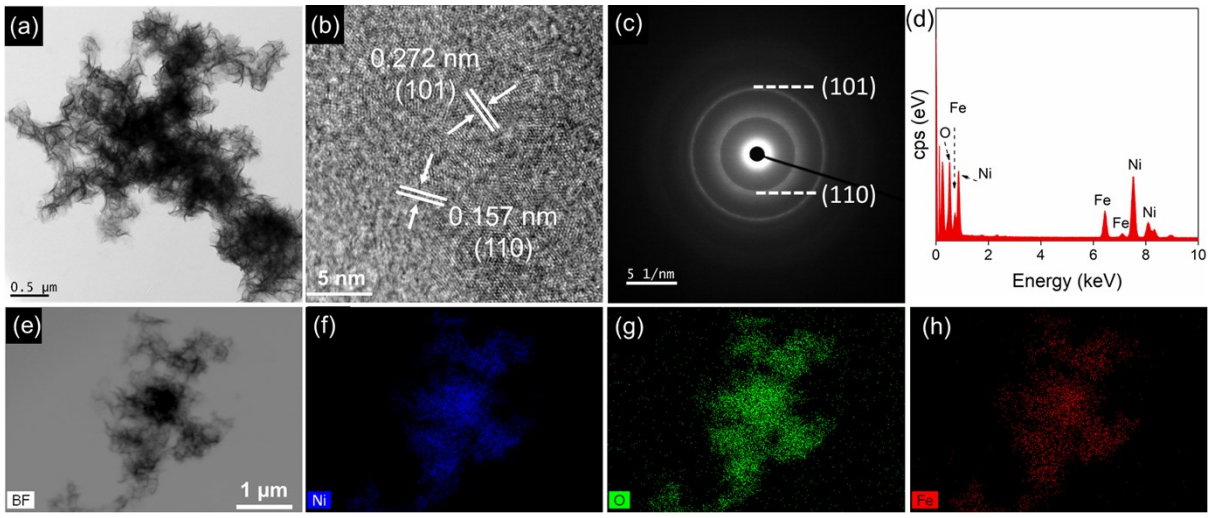

Fig. S4 (a) TEM, (b) HRTEM images and (c) SEAD patterns of NiFe-OH. EDX elemental mapping of Ni-OH: (d) the corresponding EDX spectrum, (e) bright-field image, (f) Ni, (g) O and (h) Fe.

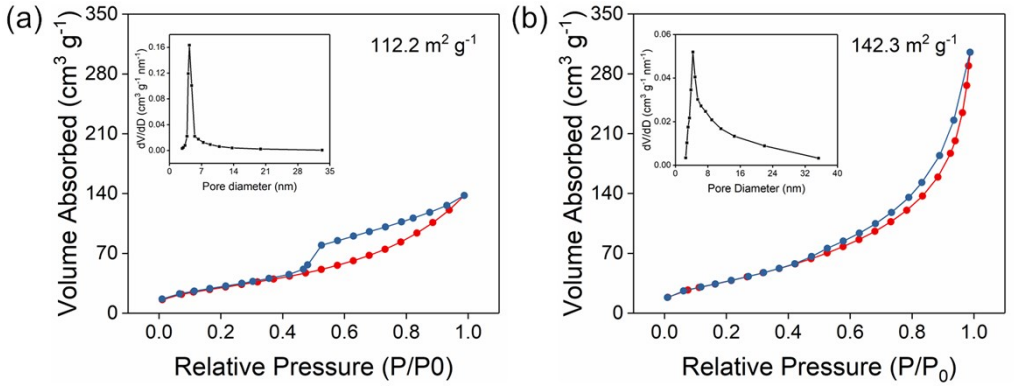

Fig. S5 N_2-adsorption-desorption isotherm curves and the corresponding pore size distribution of (a) Ni-OH and (b) NiFe-OH.

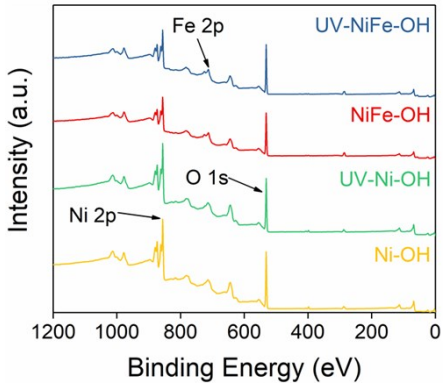

Fig. S6 Survey scan of Ni-OH, UV-Ni-OH, NiFe-OH and UV-NiFe-OH.

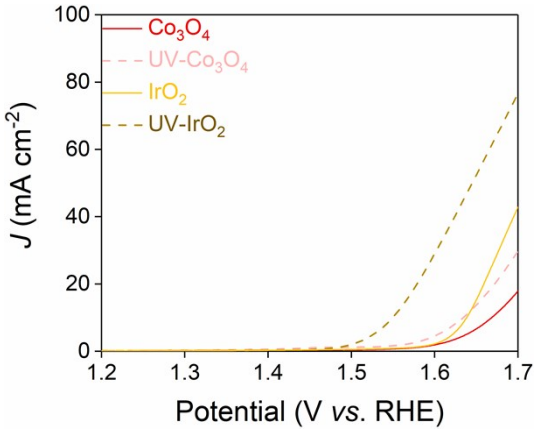

Fig. S7 LSV curves of commercial IrO_2 and lab synthesized Co_3O_4 for OER at a scan rate of 5 mV s^{-1}.

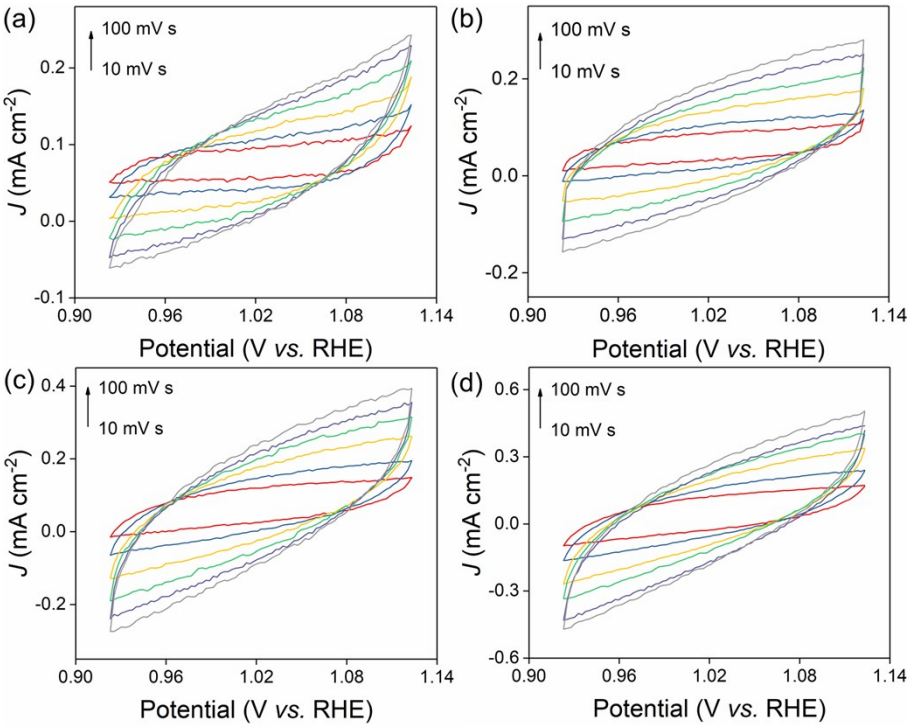

Fig. S8 CV curves of (a) Ni-OH, (b) UV-Ni-OH, (c) NiFe-OH and (d) UV-NiFe-OH.

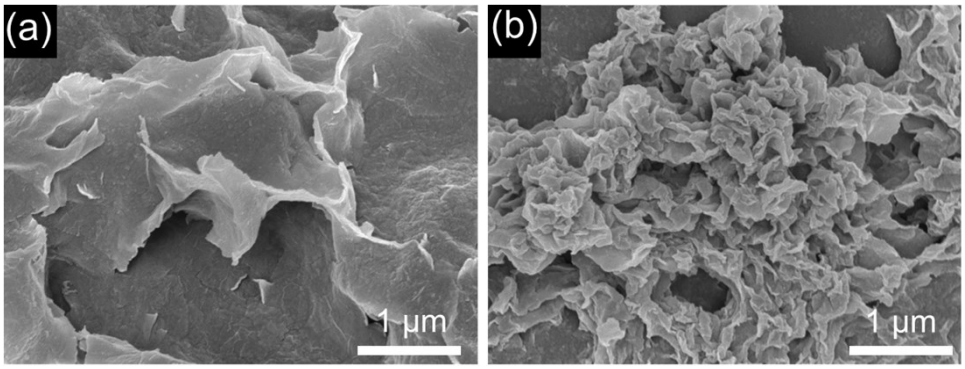

Fig. S9 SEM images of UV-Ni-OH and UV-NiFe-OH after stability test.

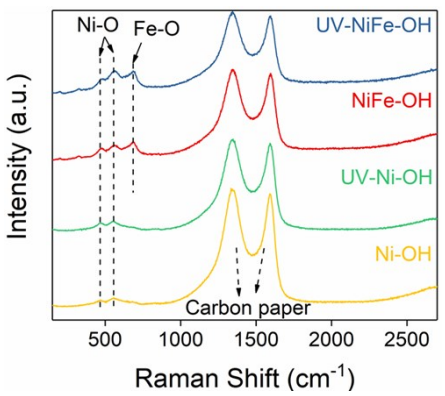

Fig. S10 Raman spectra of (a) Ni-OH, (b) UV-Ni-OH, (c) NiFe-OH and (d) UV-NiFe-OH after stability test.

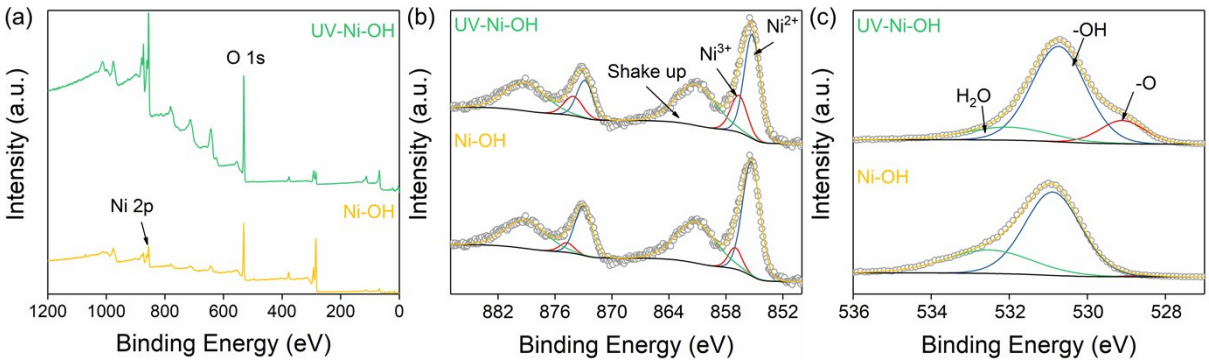

Fig. S11 XPS spectra of (a) survey scan, (b) Ni 2p and (c) O 1s for Ni-OH and UV-Ni-OH after stability test.

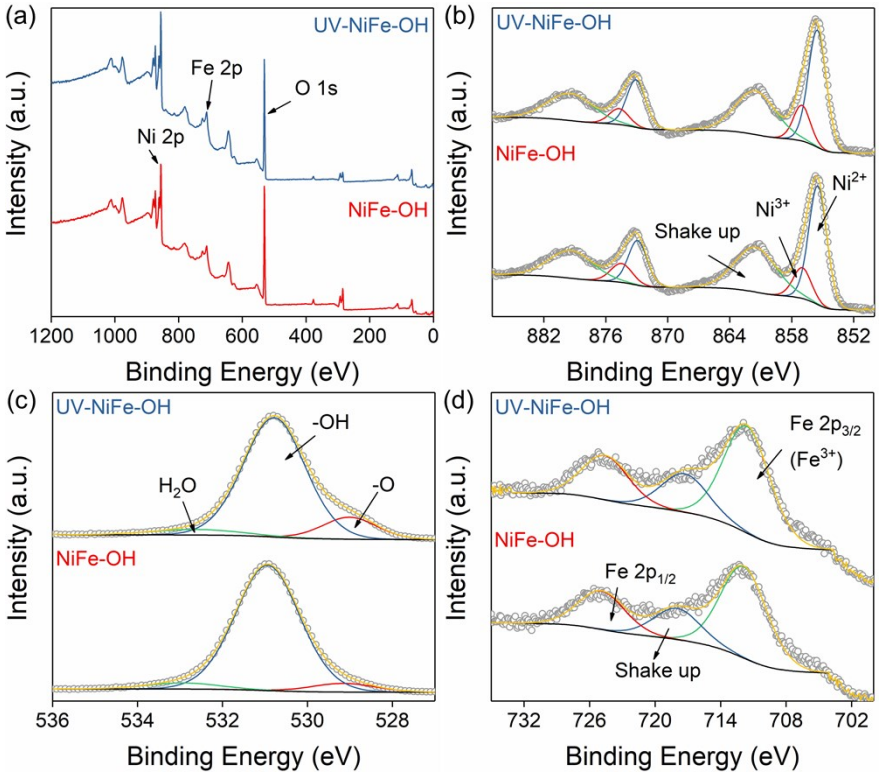

Fig. S12 XPS spectra of (a) survey scan. (b) Ni 2p, (c) O 1s and (d) Fe 2p for NiFe-OH and UV-NiFe-OH after stability test.

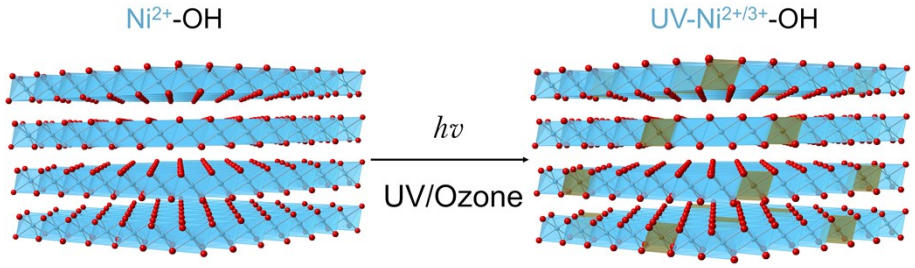

Figure S13 Crystal structures of Ni-OH (left) and UV-Ni-OH (right).

Table S1 Comparison of the OER performance of various Fe-Ni-based electrocatalysts tested in 1 M KOH electrolyte.

Catalysts	Current Density (mA cm^{-2})	Overpotential (mV)	Tafel slope (mV dec^{-1})	Ref.
FeCoNi-LTH/$NiCo_2O_4$/CC	50	302	72	[4]
$Ni_{1-x}Fe_x$-LDH	50	297	72	[5]
Co/Ni$(BDC)_2$TED	50	287	76	[6]
NiFe-LDH	30	280	50	[7]
NiFe-OH-PO_4/NF	20	249	42	[8]
Holy β-Ni$(OH)_2$	10	335	65	[9]
NiFe LDH@HPGC	10	265	56	[10]
$Ni_{0.83}Fe_{0.17}(OH)_2$	10	245	61	[11]
NiCoON	10	247	35	[12]
NiFe-NC	10	271	48	[13]
α-Ni$(OH)_2$	10	331	42	[14]
NiFe-LDH	10	250	69	[15]
UV-NiFe-OH	20	236	41	**This work**
	30	272		
	50	297		

Table S2 ECSAs calculated from C_{dl}.

Sample	C_{dl} (mF cm^{-2})	ECSA (cm^{-2})
UV-NiFe-OH	3.24	81.0
NiFe-OH	2.58	64.5
UV-Ni-OH	2.16	54
Ni-OH	1.31	32.7

Reference

1. H. Du, Y. Pan, X. Zhang, F. Cao, T. Wan, H. Du, R. Joshi and D. Chu, *Nanoscale Adv.*, 2018.
2. R. D. Smith, M. S. Prévot, R. D. Fagan, S. Trudel and C. P. Berlinguette, *J. Am. Chem. Soc.*, 2013, **135**, 11580-11586.
3. H. Du, T. Wan, B. Qu, F. Cao, Q. Lin, N. Chen, X. Lin and D. Chu, *ACS Appl. Mater. Interfaces*, 2017, **9**, 20762-20770.
4. Y. Liu, Y. Bai, Y. Han, Z. Yu, S. Zhang, G. Wang, J. Wei, Q. Wu and K. Sun, *ACS Appl. Mater. Interfaces*, 2017, **9**, 36917-36926.
5. G. Rajeshkhanna, T. I. Singh, N. H. Kim and J. H. Lee, *ACS Appl. Mater. Interfaces*, 2018, **10**, 42453-42468.
6. D.-J. Li, Q.-H. Li, Z.-G. Gu and J. Zhang, *J. Mater.Chem. A*, 2019, **7**, 18519-18528.
7. Z. Lu, W. Xu, W. Zhu, Q. Yang, X. Lei, J. Liu, Y. Li, X. Sun and X. Duan, *Chem. Commun.*, 2014, **50**, 6479-6482.
8. Z. Lei, J. Bai, Y. Li, Z. Wang and C. Zhao, *ACS Appl. Mater. Interfaces*, 2017, **9**, 35837-35846.

9. X. Kong, C. Zhang, S. Y. Hwang, Q. Chen and Z. Peng, *Small*, 2017, **13**, 1700334.
10. Y. Ni, L. Yao, Y. Wang, B. Liu, M. Cao and C. Hu, *Nanoscale*, 2017, **9**, 11596-11604.
11. Q. Zhou, Y. Chen, G. Zhao, Y. Lin, Z. Yu, X. Xu, X. Wang, H. K. Liu, W. Sun and S. X. Dou, *ACS Catal.*, 2018, **8**, 5382-5390.
12. Y. Li, L. Hu, W. Zheng, X. Peng, M. Liu, P. K. Chu and L. Y. S. Lee, *Nano Energy*, 2018, **52**, 360-368.
13. A. Kumar and S. Bhattacharyya, *ACS Appl. Mater. Interfaces*, 2017, **9**, 41906-41915.
14. M. Gao, W. Sheng, Z. Zhuang, Q. Fang, S. Gu, J. Jiang and Y. Yan, *J. Am. Chem. Soc.*, 2014, **136**, 7077-7084.
15. D. Zhou, X. Xiong, Z. Cai, N. Han, Y. Jia, Q. Xie, X. Duan, T. Xie, X. Zheng and X. Sun, *Small Methods*, 2018, **2**, 1800083.